

6. Non-linear and nonstationary processes in geodetic TD/WV

*So, Nat'ralists observe, a Flea
Hath smaller Fleas that on him Prey,
And these have smaller Fleas to bit' em,
And so proceed, proceed ad infinitum*
- J'onathan Swift (1667-1745)

This Chapter presents results and discussion on the non-linear properties in the fluctuations of TD/WV based on the statistical information derived from DFA. In order to account for the non-linear and nonstationary properties in TD/WV fluctuations, the EMD/EEMD is used. Self-similar behaviour in TD/WV is assessed and found to be present. The lasting periods of synchronization with fluctuating phase coincidence (and correlations by pairs thereof) between different oscillation modes of WV and atmospheric mean temperature demonstrate that fluctuations (which are non-linear and depicted in the phase shifts) in WV and temperature are driven by common underlying processes (exhibiting possible stochastic resonance). Assessing the significance of non-linearity and nonstationarity in geodetic data analysis is demonstrated by the introduction of non-linear function to account for azimuth dependent atmospheric range correction. Using a one-month SLR data, more than 15% improvement of the O-C residuals is achieved for both LAGEOS 1 and 2.

6.1. Introduction

In the research reported in this Chapter, the emphasis is on the analysis of the variability of geodetic tropospheric parameters by extracting the local time/frequency scales of variability embedded in the geodetic time series. A data adaptive decomposition (by using the EMD and/or EEMD) is considered, whereby complete, orthogonal and local components are obtained. Often EMD/EEMD decomposes the time series into IMF according to the levels of their local oscillation or frequency. The EMD effectively captures the non-linear characteristic in respect of the amplitude and frequency modulation with local time scales. In

this regard, the local time/frequency scales are defined by the instantaneous frequency. Once IMFs are obtained, Hilbert Transform spectral analysis is performed on the time series to provide the temporal-frequency variation of information which is a key component of time-frequency analysis for nonstationary geodetic-tropospheric time series.

In particular, a non-decimated Haar wavelet transform and EMD/EEMD are used to analyse nonstationary processes in WV and other derived tropospheric parameters such as tropospheric delay due to WV. In the first part, geodetic WV measured at HartRAO is tested for nonstationarity and non-linearity using DFA in the wavelet space. Here the geodetic WV was decomposed into the wavelet space and thereafter, the characteristic fluctuation properties of the power spectra are investigated using DFA. Furthermore, the EEMD was used for correlation analysis of some of the important tropospheric parameters such as wet zenith delay and mean tropospheric temperature that affect the accuracy of the geodetic delay observable over geodetic stations; here, we have used the geodetic station at HartRAO, South Africa. The correlation analysis considered here illustrate the synchronisation or the degree of closeness of the modes in WV and mean atmospheric temperature time series derived from the phase variance between the time series (Botai *et al.*, 2009b).

6.2. Nonstationary processes in tropospheric WV using wavelet analysis

Non-linear processes exist in nature; examples of the dynamical systems that exhibit non-linear and nonstationary characteristics include the Earth's climate system (Rial *et al.*, 2004), river flow and discharge (Montanari *et al.*, 2000), atmosphere (Ivanova, *et al.* 1999; Ausloos *et al.*, 2001). If a geophysical field such as PWV is decomposed additively into structural components such as the trend, the cyclical and seasonal and irregular components, then the coherence between the properties of the observed PWV series and those of the structural components could be assessed. The characteristics structure in the components of the time series could be used to evaluate nonstationarity manifested in the second order properties such as the variance and the mean. This may be an indication that the dynamical processes in the geophysical field are driven by complex processes as reported by Taqqu *et al.*, (1995), Verdes *et al.*, (2001) and Hu *et al.*, (2001).

In the current analysis, the presence of memory in the tropospheric PWV is assessed using statistical theory. Using a global PWV parameter (gPWV) estimated at HartRAO, the PWV time series during 2000-2006 was reconstructed with sliding window using Singular

Spectrum Analysis (SSA). See Ghil *et al.*, (2001) for a detailed account on SSA. The gPWV is defined (here) as the daily mean PWV value computed from two geodetic techniques (GPS and VLBI) and NWP models. The wavelet transform of the reconstructed gPWV time series was computed using the non-decimated Haar wavelet technique (Percival *et al.*, 2000). As described in Chapter 3, the presence of discontinuities due to boundaries in the data is accounted for by reflecting the time series onto the last observation. This method of handling discontinuities in the geodetic PWV is tractable because the sample mean and variance are not affected and the seasonal patterns in PWV time series exhibits are preserved.

The DFA and wavelet joint estimator were used to calculate the second-order parameters (e.g., the mean, variance and scaling exponent measure the scaling behaviour) that are used to infer the (non-)stationary properties in the reconstructed time series. The purpose of wavelet joint estimator is to eliminate the deterministic trends and non-discontinuous changes in the second-order properties in the WV fluctuations.

Figure 6.1 depicts the reconstructed gPWV computed from leading principal components projected onto a reduced subspace with minimum redundancy in SSA. In this way, the gPWV was smoothed and any noise in the time series eliminated through filtering. This method of filtering preserves the second order statistical parameters which characterise nonstationarity and/or local stationarity.

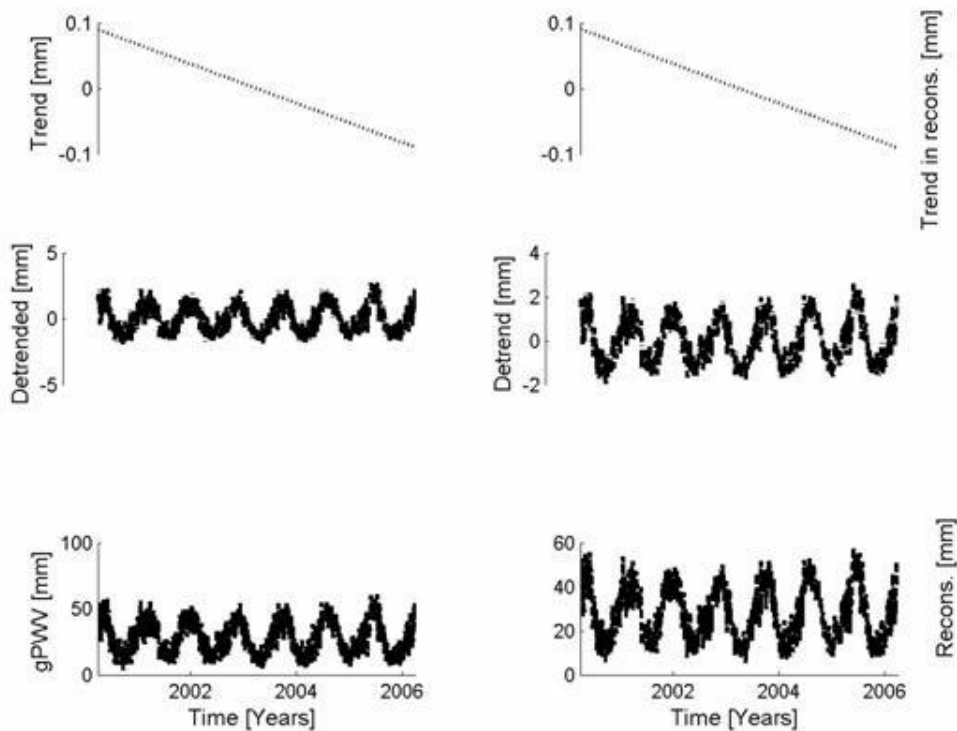


Figure 6.1. PWV time series. Left: Non-detrended PWV time series. Right: PWV derived from the singular spectrum analysis.

Figure 6.2 depicts the 'detail' (even scales) of the gPWV in the wavelet space derived from the Maximum Overlap Discrete Wavelet Transform (MODWT) analysis (see Whitcher 1998; Percival *et al.*, 2000). The MODWT technique allows the non-linear and nonstationary structure (e.g., trends, jumps and spikes) in the data to be examined in the wavelet space. The illustrated temporal scales correspond to the physical time scales 1 week, 2 month, 4 months, and 8 months respectively. In order to get a better understanding of the inherent PWV fluctuation patterns, the individual frequency levels are separated out and plotted as functions of time as shown in Figure 6.2. Each frequency band spans over the time span with gradual decreasing time resolution. From Figure 6.2, we suppose that some contaminating observations other than the gPWV observations (the outliers) are embedded in the high modes of oscillations (Greenblatt, 1994). Therefore caution should be taken when interpreting the oscillatory components, especially the high frequency wavelength coefficients. It is evident from Figure 6.2 that gPWV exhibits temporal nonstationary characteristics.

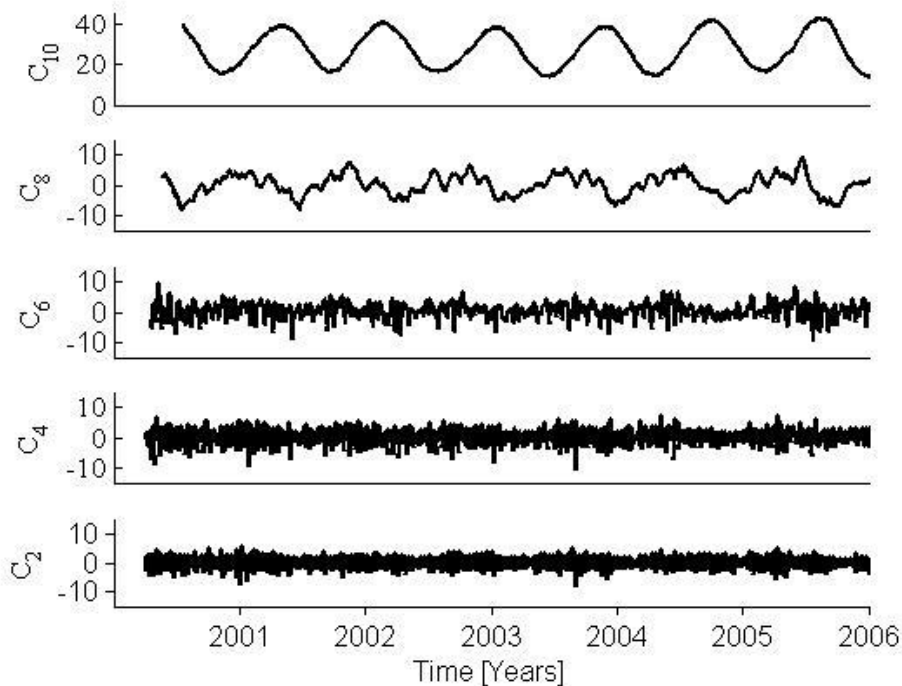


Figure 6.2. Haar wavelet spectra of the reconstructed gPWV at different even-scales.

In order to study some aspects of self-similar behaviour present in the reconstructed gPWV times-series, local linear least square function was fit to a standardised integrated time series constituted from segments of gPWV. The average fluctuation for each segment was used to compute the scaling exponent. Figure 6.3 indicates that a single linear fit on the gPWV power spectral density has different values of β at different scales (the wavelet scale and β are linearly dependent). As depicted in Figure 6.3, the SS and LRD measures are dependent on the 'detail' of WT.

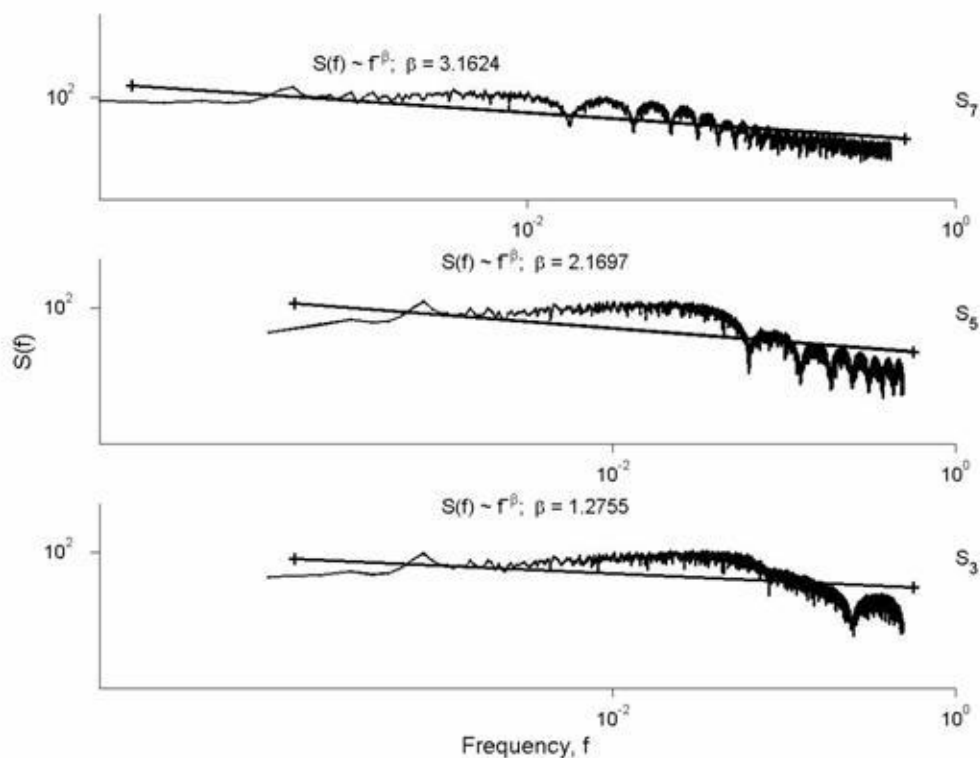


Figure 6.3. The power spectral density of gPWV at different scales.

Figure 6.4 illustrates that the root mean square fluctuations and the sliding window width have different scaling exponents (α), suggesting that the long-range power-law correlation in gPWV (i.e. $\alpha > 0.5$) is dependent on the physical time scales. These results indicate that atmospheric processes manifested in the PWV fluctuations are long-range correlated.

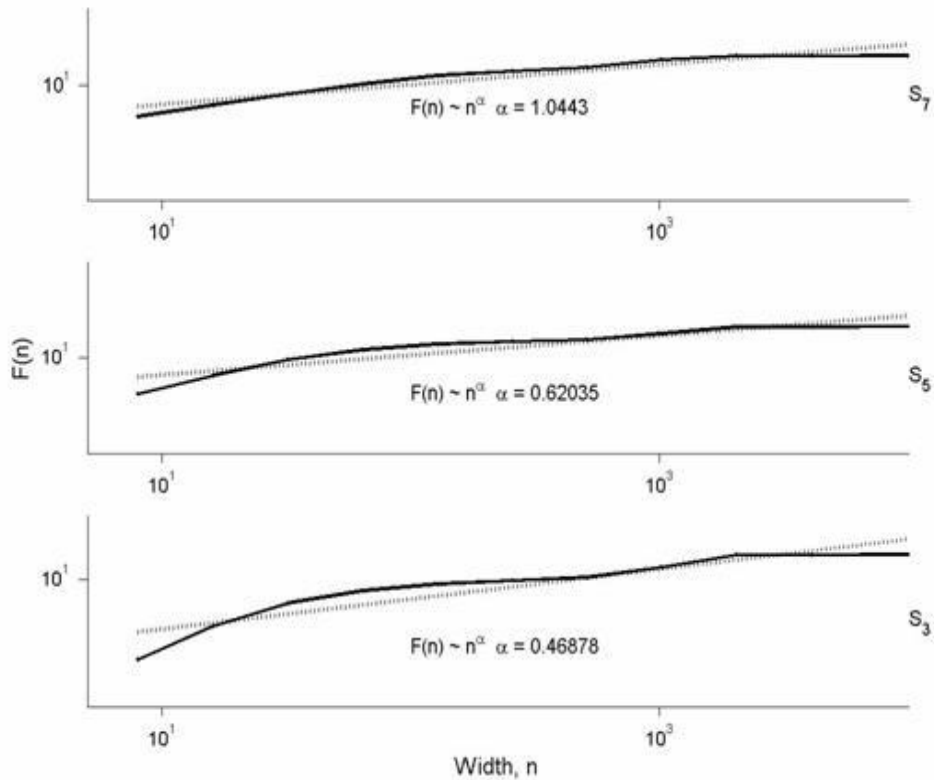


Figure 6.4. Scaling behaviour of the reconstructed gPWV time Series.

The temporal variation of the mean, variance and α of gPWV is depicted in Figure 6.5. The temporal variation in the mean and variance (and also correlations) can be used to measure the presence of SS and/or LRD. In our analysis using the wavelet estimator of Abry and Veitch, (1998) of second-order parameters, the test for SS and/or LRD properties in gPWV time-series showed that the mean and variance are not time invariant as illustrated in Figure 6.5. The experimental analysis for stationarity reported here considered four vanishing moments, the sub-series scale $j_{1,2} = \{2:4\}$ while the scales for the whole series was set to $j_{1,2} = \{2:8\}$. This shows that tropospheric PWV has SS and LRD properties.

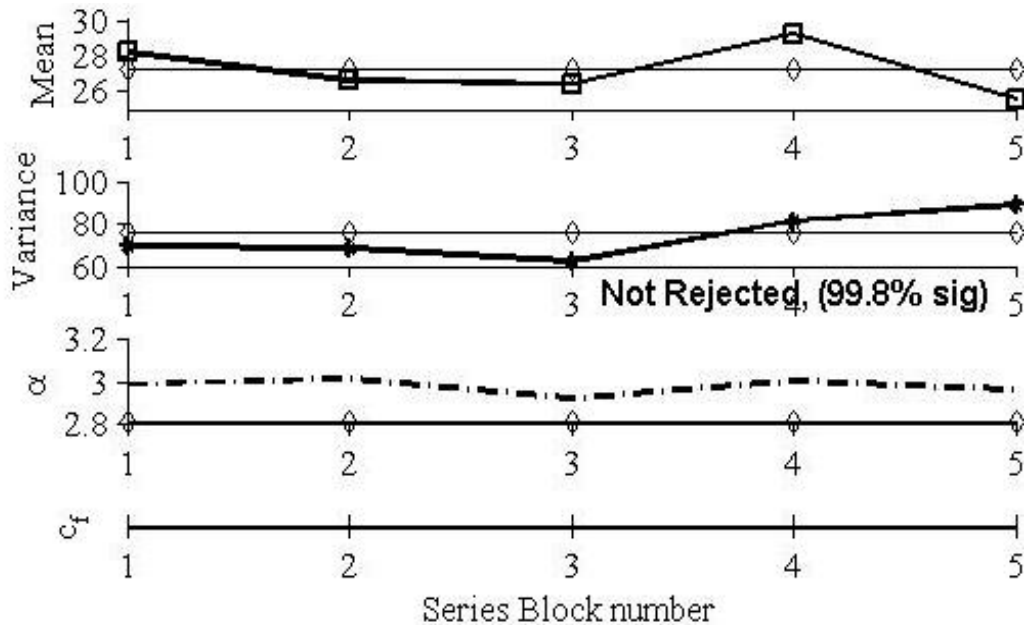


Figure 6.5. Wavelet estimator for SS and LRD at the 10th scale.

6.3. On the noise-Assisted geodetic data analysis

Analysing non-linear and nonstationary data series using the HHT is a new cutting-edge methodology that is widely used in many scientific fields such as finance (e.g., Huang *et al.*, 2003b), biomedical applications (e.g., Huang *et al.*, 1999b), natural sciences (e.g., Salisbury and Wimbush 2002; Pan *et al.*, 2002) and engineering sciences (e.g., Huang *et al.*, 2005). For example, Salisbury and Wimbush,(2002) used Southern Oscillation Index (SOI) data and applied the HHT technique to determine whether the SOI data are sufficiently noise free; if useful predictions can be made and whether future ENSO events can be predicted from SOI data. Pan *et al.*, (2002) used HHT to analyse satellite scatterometer wind data over the North-Western Pacific and compared the results to Vector Empirical Orthogonal Function (VEOF) results. More recently, Pegram *et al.*, (2008) suggested an improvement to the original EMD algorithm using rational splines and the flexible treatment of the end conditions and applied it to rainfall time series analysis.

Figure 6.6 depicts the temporal variations of the daily-averaged WV, zonal and meridional gradients derived from ECMWF data at HartRAO over the period from 2006-2009. From Figure 6.6, it is evident that the WV and linear horizontal gradients time series show that fluctuations occur on time scales much shorter than the length of the entire time series. The short-time fluctuations are then decomposed into IMFs. In this report, IMFs derived from WV daily time series data are given in Figure 6.7. The current WV data resulted

in 11 IMFs (the trend inclusive). These oscillations are not visible in the WV raw data due to their superposition. Looking at individual IMFs, it is possible to decipher information regarding WV variability at different time-scales. In particular, δ_{3-5} clearly shows intra-seasonal modes whose period of oscillation varies from days to months. However, δ_6 shows an almost periodic envelope with amplitudes having seasonal dependence. When examining the low frequency modes of WV fluctuations depicted in Figure 6.7, we notice that δ_8 exhibits regular intra-annual fluctuations that corroborate with the sub-tropical seasons. This component is also visible in the raw WV data.

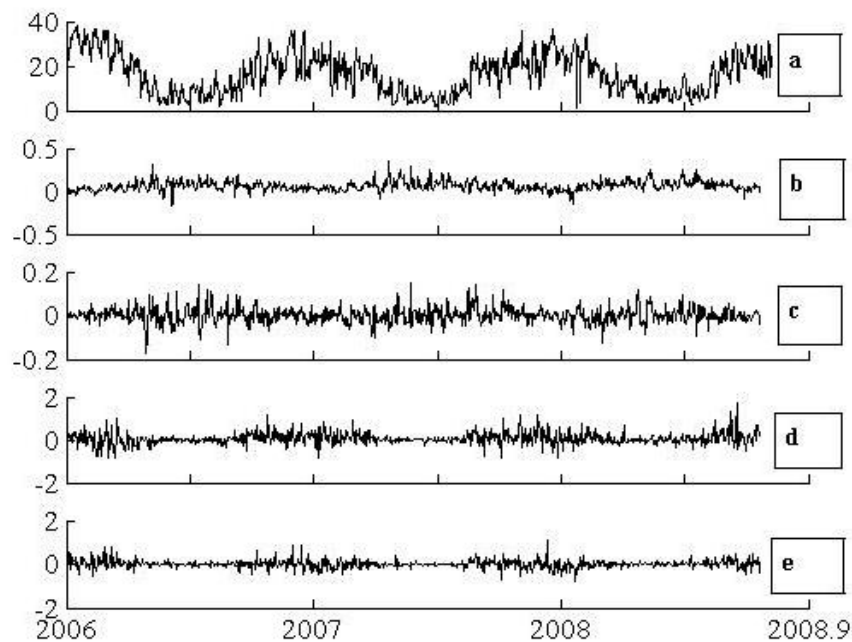


Figure 6.6. Time series (time is plotted in the x-axis) of a) Water vapour, mm; b) Meridional hydrostatic; c) Zonal hydrostatic; d) Meridional wet and e) Zonal wet; linear horizontal gradients, mm/degree.

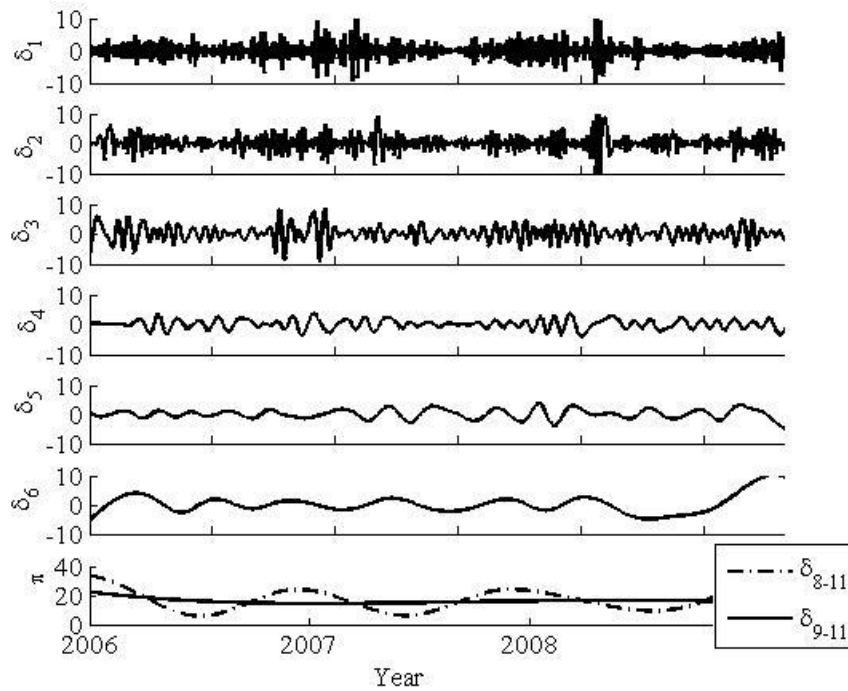


Figure 6.7 WV derived IMFs ($\delta_{1 \rightarrow 6}$). The bottom panel illustrates the adaptive trends.

Given that the trend is a local non-oscillatory function defined for a local time scale, the trend is also one of the many local properties of the data, (see Zhaohua *et al.*, 2007). From the tropospheric WV, we see oscillatory modes are superimposed onto a monotone (oscillatory and decreasing) base function. In particular, various trends such as diurnal, intra-annual and annual trend are plotted in Figure 6.8. From Figure 6.8, the overall adaptive trend (π_{11}) is approximately identical to the linear trend (see bottom panel). The overall adaptive trend is derived from the entire data span. Annual and intra-annual trends are formed from the combination of trends derived from δ_{8-11} IMFs.

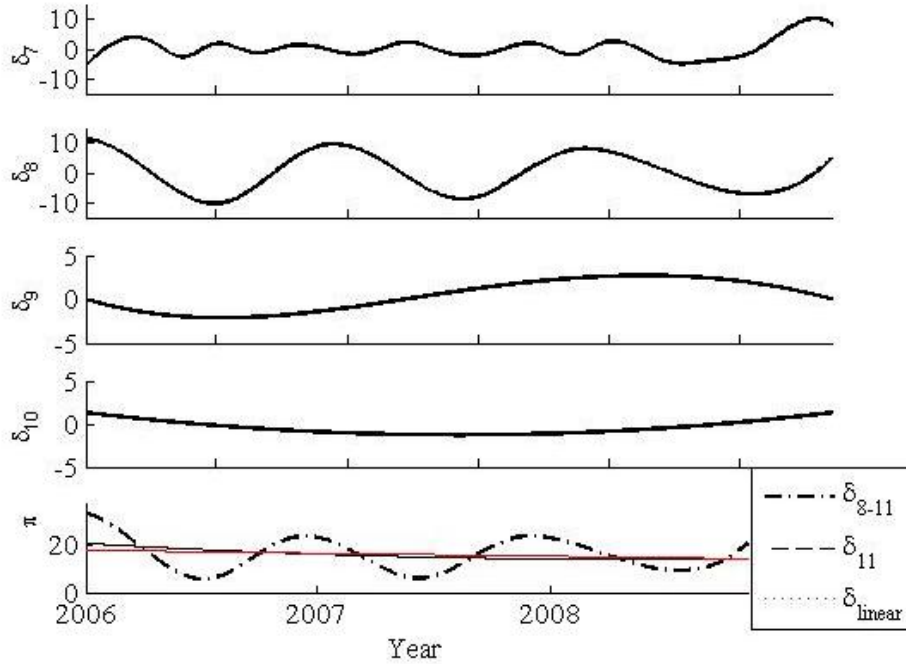


Figure 6.8. Low frequency IMFs and linear and adaptive trends at different time scales.

To completely characterise the tropospheric WV and linear horizontal gradients fluctuations, local time/frequency scales (defined by the instantaneous frequencies of IMFs) of the decomposed time series were extracted. The instantaneous frequencies of the 6th IMF for WV and the zonal linear horizontal (hydrostatic and wet) gradients are plotted in Figure 6.9.

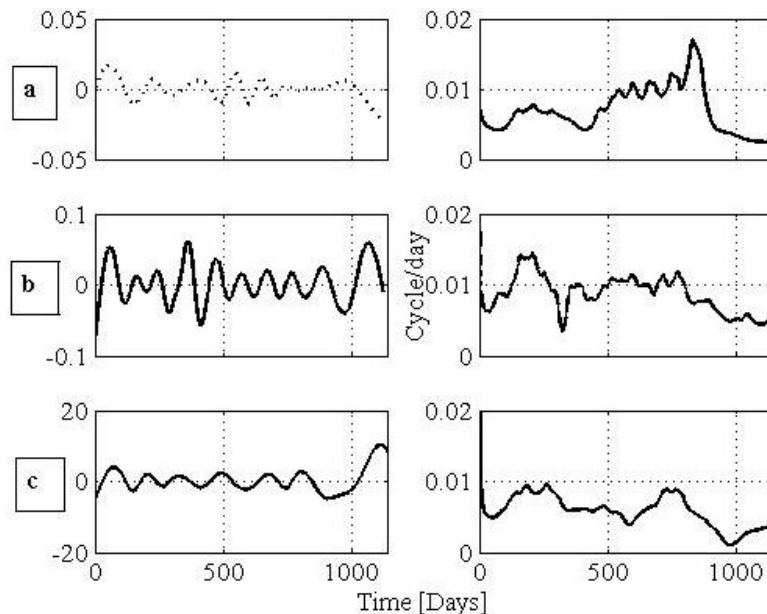


Figure 6.9. The Instantaneous frequency of the 6th IMF. From top left to right: a) Zonal hydrostatic gradient and instantaneous frequency, b) Zonal wet gradient and instantaneous frequency and c) WV and instantaneous frequency.

The probability distribution of individual IMFs examined using WV and the linear horizontal components. The results show that the probability distribution is approximately normally distributed (see Figure 6.10 to Figure 6.12; the fitted normal distribution curve is also depicted). From the current variables, it can be noticed that, the first three IMFs derived from WV, hydrostatic and zonal linear horizontal gradients exhibit normal probability distribution. These results are consistent with those reported in Wu and Huang, (2004) and they are also in agreement with the central limit theorem.

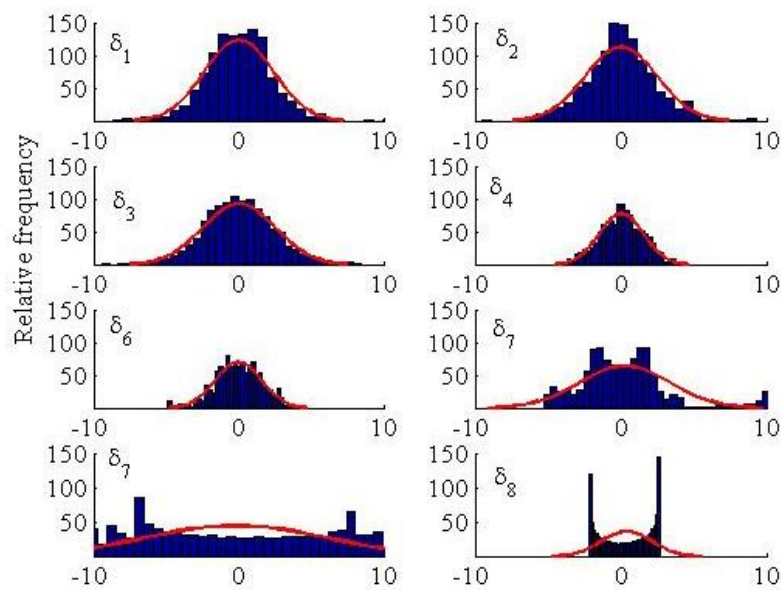


Figure 6.10. Probability distribution of WV derived IMFs.

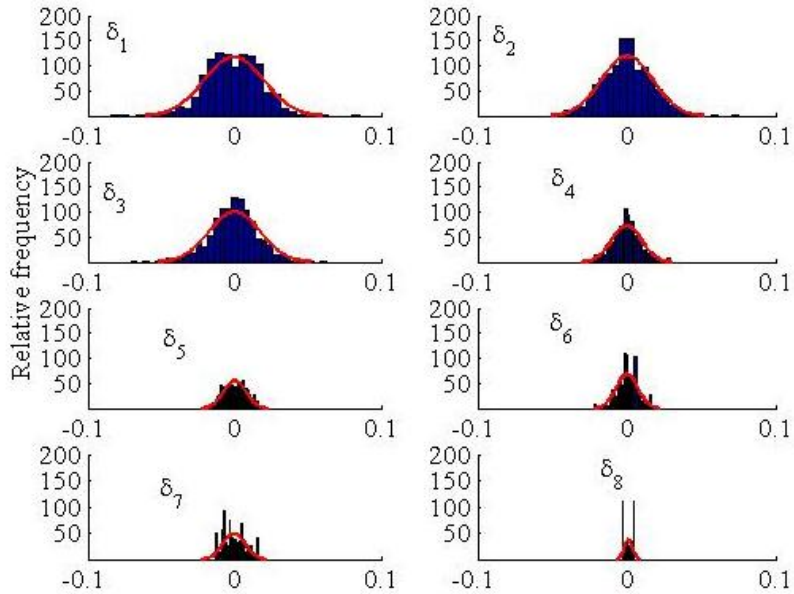


Figure 6.11. Probability distribution of the zonal linear horizontal hydrostatic gradients.

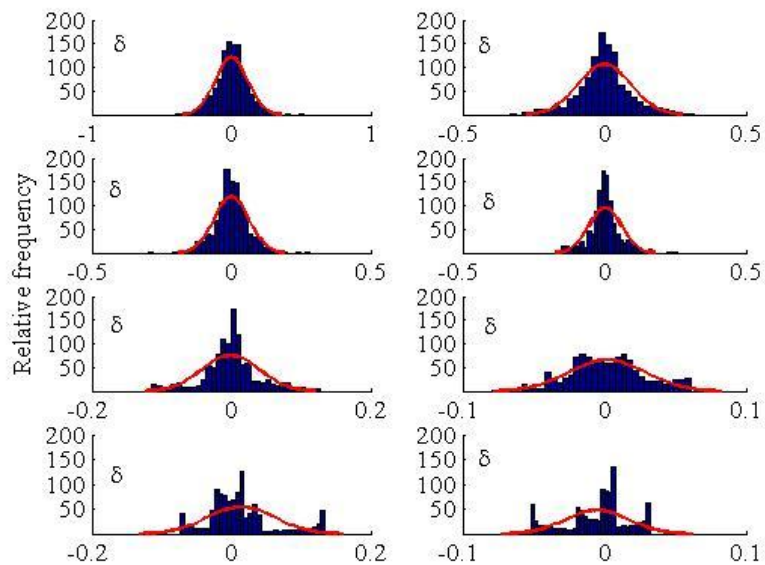


Figure 6.12. Probability distribution of the zonal linear horizontal wet gradients.

From the probability distribution depicted above, it can be observed that the deviation from the normal distribution function increases with an increase in the frequency modes of WV and linear horizontal gradients. This behaviour could be attributed to the decrease in the number of oscillations which reduces the ensemble sample size and therefore results in the less smooth distribution. Higher number of oscillations (number of IMFs with high frequency modes) follows the normal distribution according to the central limit theory. Following

Papoulies, (1996), it could be expected that WV and linear horizontal gradients therefore exhibit a Chi-square distribution.

The combination of EMD and Hilbert spectrum analyses provides an alternative adaptive method to analyse nonstationary and non-linear time series. It can perform and enhance most of the traditional data analysis tasks, such as filtering, regressions, and spectral analysis adaptively. To accommodate data from nonstationary processes, a number of methods such as spectrogram, Wigner- Ville distribution, and Wavelet analysis have all been used extensively with some degree of success. Recently, the EMD method has attracted considerable attention and been used widely in many fields. While the EMD methodology has proved to be versatile and robust, it cannot reveal the signal characteristic information accurately. This is because it has a shortcoming of mode mixing; a condition where an IMF exhibits local oscillations with clear different time/frequency scales, as reported in Huang *et al.*, (1999). A solution to this problem is by subjectively introducing constraints for mode mixing, which eliminates the adaptability property in the EMD data.

Geodetic data is often measured at different spatial-temporal scales. On decomposing the intermittent sampled geodetic data, the resultant IMFs exhibits scales with a broad spectrum or redundant signals. This condition causes aliases in the time-frequency distribution. Redundancy in IMFs oscillations often conceals important characteristics that depict physically meaningful information in the data. To alleviate the mode mixing problem occurring in EMD, the EEMD method is applied. With EEMD, the components with a truly physical meaning can be extracted from the signal.

A finite, non-infinitesimal and amplitude white noise is used to force the ensemble to exhaust all possible solutions in the sifting process, thus require different scale signals to collate in the proper IMF dictated by the dyadic filter banks (Zhaohua and Huang, 2009). The effect of the added white noise is to present a uniform reference frame in the time-frequency and time-space. This implies that the added noise provides a natural reference for the signals of comparable scale to collate in one IMF. With this ensemble mean, the scale can be clearly and naturally separated without any priori subjective criterion selection, such as in the intermittence test for the original EMD algorithm. This new approach fully utilises the statistical characteristics of white noise to perturb the data in its true solution neighbourhood and then cancel out through the ensemble averaging.

6.3.1. Correlation of tropospheric WV and temperature using phase differences

Variability of troposphere WV and mean temperature plays an important role in driving the global energy and water cycles. In space geodesy, WV and temperature affect the accuracy of the delay observable. It is therefore important to study the temporal correlations of WV and temperature to understand the bias contribution from each of these parameters to the geodetic delay observable. A flexible methodology for analysing the WV fluctuations and mean temperature that adapts to their noise and uneven spectral measurements is reported in this section. The correlation strategy employed here involves the linkage of instantaneous phase differences among the associated WV and temperature IMF modes derived from the EEMD.

In this particular analysis, the amplitude level of the first IMF is taken as reference amplitude for the noisy IMFs in the data. The assumption taken here is that, the first IMF (with highest frequencies) is corrupted with noise. Therefore the criterion for selecting meaningful empirical IMFs is based on the proportion amplitude of target IMF to the reference amplitude where the amplitude of the selected amplitude ought to be about 25% of the maximum amplitude of the reference IMF. The rationale behind this criterion is derived from the relationship between the IMF amplitude and the total energy of the IMF which is the square of the amplitude is the equivalent to the energy of the IMF. As a result, the analysis uses only significant oscillating IMFs.

The phase differences between the selected IMF derived from WV and calculated temperature, provides the degree of linkage between different modes of the respective IMFs. Using the Hilbert transform, local frequencies of each IMF mode can be computed by using Equation (122). In this research, the focus is projection of the phase shift defined by Equation (122)

$$\varpi_{i,j}^t = \Re\left(e^{i\Delta\theta_{i,j}^t}\right) \quad (122)$$

where $\Delta\theta_{i,j}^t = |\theta_i^t - \theta_j^t|$. To determine the closeness of the modes, a global indicator of the constant phase shift between WV and temperature: the variance of $\varpi(\cdot)$ is computed. The constraint used to detect pairs of modes with constant phase shift in this study is that of $\text{var}[\varpi(\cdot)] \leq 0.33$. Thereby, the IMFs with $\text{var}[\varpi(\cdot)] \geq 0.33$ have different local frequencies and hence have weak or no correlation.

Raw daily WV and mean atmospheric temperature data corresponding to the atmosphere over HartRAO exhibits certain unusual magnitudes (see Figure 6.13) due to systematic or instrumental errors. These errors were filtered out by ensuring that the data sets have been pre-processed using the adaptive filtering procedure as described in Chapter 3 prior to the IMFs extraction. The adaptive filtering stage also gives more stability to the produce IMFs extraction. The adaptively filtered time series data are plotted in Figure 6.13. In the figure, time is expressed in days since January 2005. The adaptive filtering procedure was done using a basic variability value of 0.08, the filter coefficient of 3.0 and 0.05 controlling coefficient. As observed from the filtered time series, there exists nontrivial structure in the WV fluctuations and mean atmosphere temperature. In Chapter 3, it is reported that data could fail a test for Gaussian, thus ruling out a Gaussian linear stochastic process as the source of fluctuations. Due to this inconsistency, application of the *model-based*¹¹ methods to assess the structure components in WV fluctuations might be not yield representative properties.

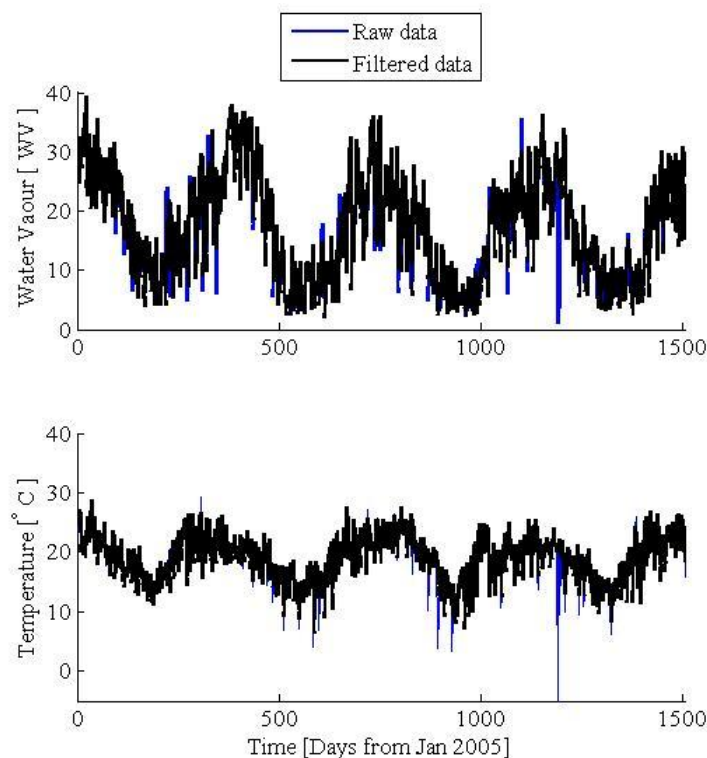


Figure 6.13. Time series of water vapour (top) and mean atmosphere temperature (bottom).

¹¹ Ad-hoc and model-based (e.g., ARMA & ARIMA) approaches are used to decompose a time series into structural components such as trend, seasonal/cyclic and irregular components.

The IMFs of WV and temperature data are shown in Figure 6.14 and Figure 6.15 respectively. The original WV and temperature data and the eight IMFs (the components from short to longer time periods) are plotted from top to bottom. Here IMF₈ corresponds to the trend in the data set.

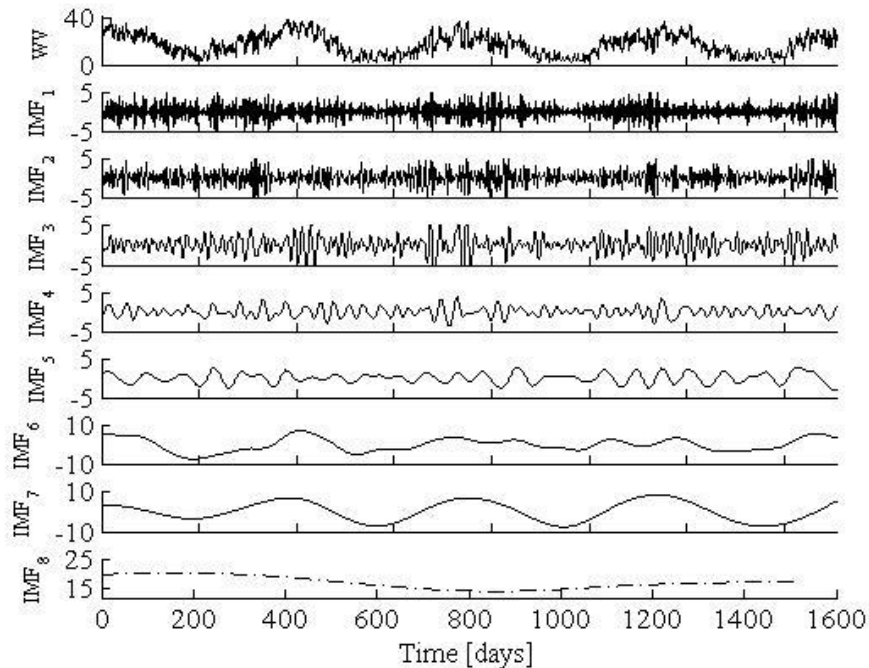


Figure 6.14. Intrinsic mode function components of water vapour over HartRAO.

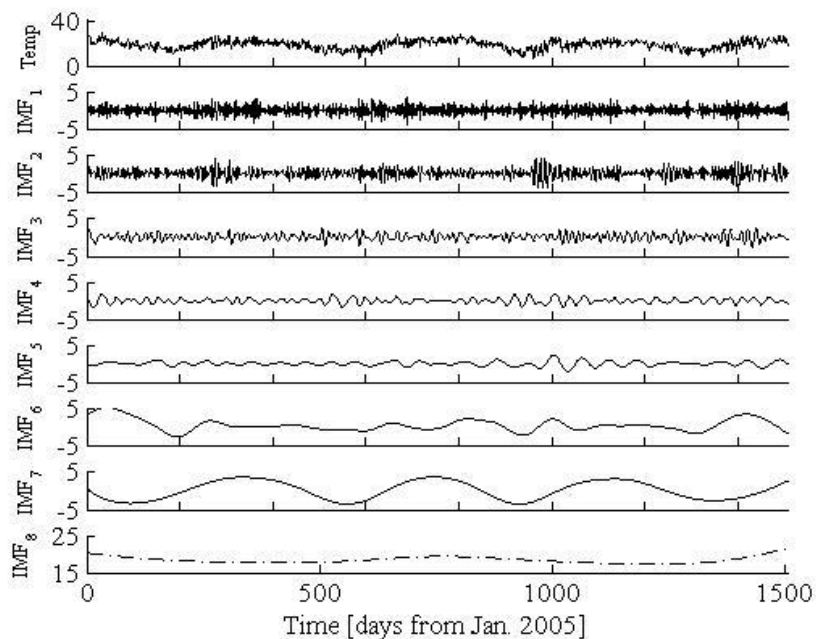


Figure 6.15. Intrinsic mode function component of mean atmosphere temperature over HartRAO.

The observed low frequency IMFs could be associated to the fluctuations that are driven by physical processes, while the high-frequency IMFs dependent on noise and independent external forces. As observed from the Figures 6.14 and Figure 6.15, the local periods are not constant but for each fixed IMF, they are constrained within different ranges. The IMFs of WV depicted in Figure 6.14 exhibits oscillation patterns with characteristic periods; annual ($IMF_{6,7}$ mode), seasonal ($IMF_{4,5}$ mode), monthly (IMF_3 mode) and diurnal ($IMF_{<2}$ mode) components. IMF_8 corresponds to the non-linear trend which exhibits both positive and negative trend. The IMF_s of the mean atmosphere temperature over HartRAO (see Figure 6.15) exhibit similar local periods ranging from 400 to 500 days ($IMF_{6,7}$ mode), 60 to 100 days (IMF_s mode), 30 days (IMF_3 mode) and diurnal ($IMF_{<2}$ mode) fluctuating components.

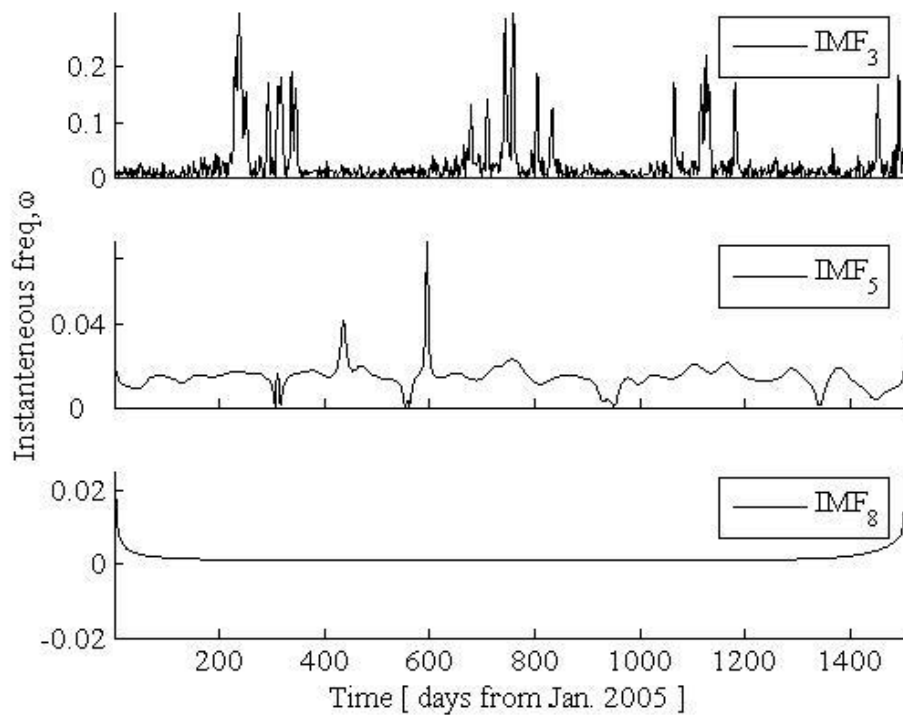


Figure 6.16. Instantaneous frequency of selected WV Intrinsic Mode Functions.

As mentioned earlier, not all the extracted IMFs from WV and mean atmosphere temperature are physically significant. Therefore on application of the criteria outlined earlier, the modes $IMF_{3,5,8}$ and $IMF_{2,5,6}$ from WV and mean atmospheric temperature respectively were considered for calculating the phase shift. As a result, Figure 6.16 and Figure 6.17 illustrate

the local frequencies of the IMFs used to derive the variance matrix for evaluating the degree of synchronisation between WV and mean troposphere temperature fluctuations. It is observed that the instantaneous frequencies (unit: cycles per day) IMF₃ and IMF₂ of WV and mean atmosphere temperature have higher values during summer months.

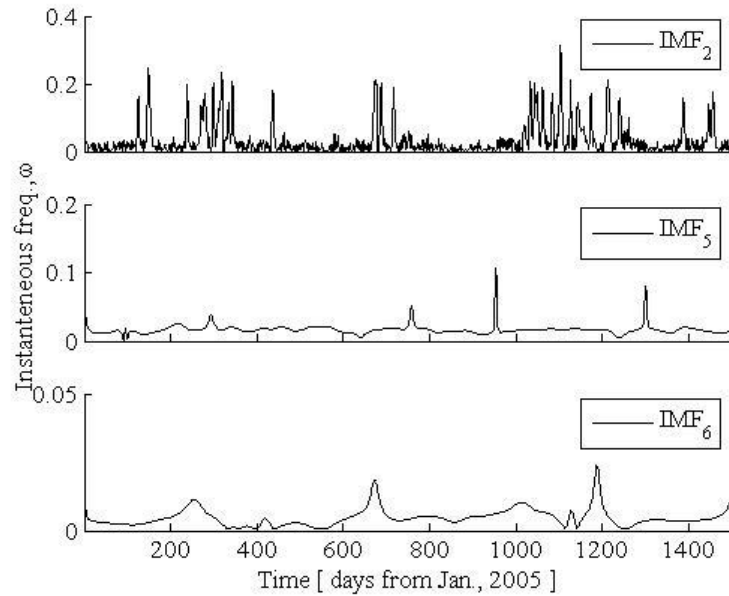


Figure 6.17. Instantaneous frequency of selected Intrinsic Mode Functions of the mean temperature.

From the variance matrix, only five pairs of modes of IMFs were considered as exhibiting lasting periods of synchronisation with fluctuating phase coincidence as illustrated in Figure 6.18. It is noted that in most of the IMFs couples selected with synchronisation, the phase coincidence fluctuates between 1 and -1 over the entire time period of this data. The correlations by pairs indicate that common fluctuations in WV and mean atmospheric temperature could be associated to both local and non-local processes. In particular, the local processes are partly responsible for driving these fluctuations i.e. heat waves and cold fronts which are common in the Highveld climatic region. The temporal dependence of phase shift seems to suggest that the WV and temperature fluctuations are strongly non-linear.. The non-linear oscillating structures visible in the phase shifts could have been triggered possibly by a stochastic resonance phenomenon such as the Inter-Tropical Convergence Zone (ITCZ) and other trade winds.

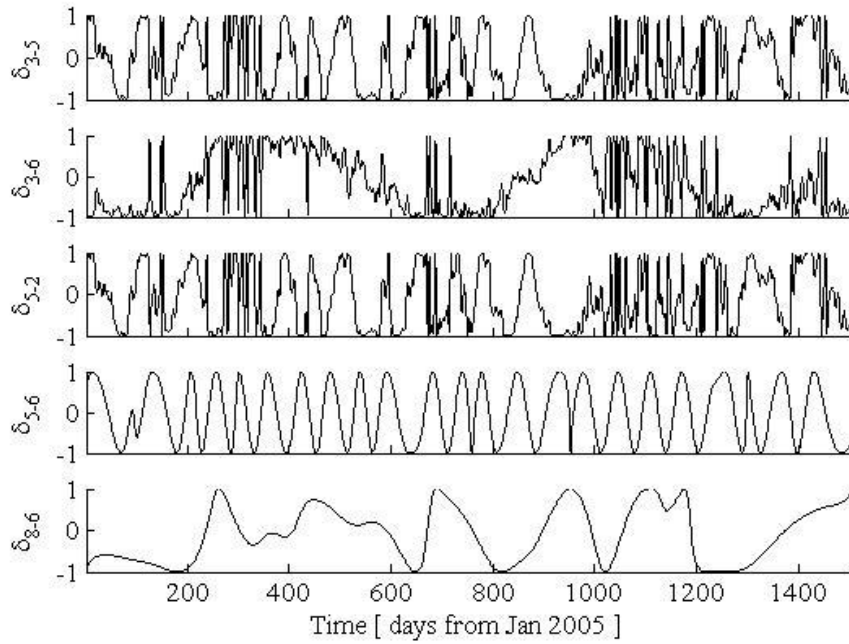


Figure 6.18. Phase shift of WV and mean atmosphere temperature IMFs modes.

6.4. Assessing the effect of non-linearity/stationarity in atmospheric range correction

Until now, the detection, analysis and characterisation of non-linearity and nonstationarity in geodetic data has been described and presented in the preceding sections of this thesis. In the present section, the benefit of introducing non-linearity and nonstationarity in atmospheric correction to the SLR range is investigated. In particular, a non-linear function is introduced to model the azimuth dependent atmospheric range correction. From the analysis of one-month of SLR data, results of azimuth dependent atmospheric range correction indicate that the introduced second-order non-linear function improves the Observed-Computed (O-C) residual by over 15%. The computed azimuth atmospheric range correction is in general negative suggesting that the current atmospheric range correction models generally overestimate the atmosphere range bias.

6.4.1. SLR atmospheric range correction

The atmosphere-Earth and Ocean is an intrinsically non-linear and nonstationary physical system that is the subject of space geodetic research. This non-linearity/nonstationarity is manifested in many series of geodetic variables depicted in Table 2.1, in Chapter 2. Detecting

and quantifying this non-linearity/nonstationarity depends on a) the type of variable, b) the geographic area and/or c) the data span. As described in the foregoing section (see Chapter 2), the range Equation used in SLR processing includes an atmospheric term which is currently modelled as an elevation only model (this is the Pavlis and Mendes (2004) model adopted by the ILRS working group). This model does not take into account the azimuth dependence and this is the point of departure. The current elevation-only model could be viewed to be linear and therefore may not be realistic since other factors such as measurement errors and unknown noise sources, may introduce non-linearities during SLR processing (and this may impact on the accuracy parameters such as station position and EOPs). In general, the measurements of e.g., the barometric pressure, temperature and relative humidity exhibit second-order terms (gradients) that are sensitive to the asymmetry of the atmosphere and could introduce some non-linearity in the atmospheric range correction term.

Detecting, characterising/analysing and incorporating non-linearity and non-stationarity into models of the SLR observation equation terms is of extraordinary importance for accurate computation of the O-C residuals. Detection and analysis of non-linearity and nonstationarity in moisture fluctuations have been achieved, in part, by calculating persistence/scaling behaviour in tropospheric delay due to WV. In order to assess the contribution of incorporating non-linear/nonstationary aspects in geodetic analysis, the current atmospheric correction used in SLR analysis has been modified by adding a non-linear term to account for the azimuth dependent atmospheric range bias. The proposed modification (see Equation (123)) has been tested on one-month of SLR data analysed by the SLR analysis software developed at HartRAO (see Combrinck, 2010).

$$O-C=R_o-\left[R_c+\Delta R_{a,e}+\Delta R_{a,az}\right] \quad (123)$$

Here, R_o and R_c are the observed and computed ranges. Similarly, $\Delta R_{a,e}$ and $\Delta R_{a,az}$ are the elevation-only and azimuth dependent (this is modelled as a second-order function) atmospheric range correction terms. There could still be remnants of other factors such as time bias and range bias; however these were estimated before the estimate of the azimuthal non-linearity so should be eliminated to a large extent.

Figure 6.19 depicts differences between O-C (for both LAGEOS 1 and 2) before and after incorporating the non-linear function. From the results, a 15 - 20% improvement in the estimated O-C derived from the analysis of one-month SLR data for the orbits of LAGEOS 1 and 2 due is attained due to incorporation of the non-linear term in Equation (123).

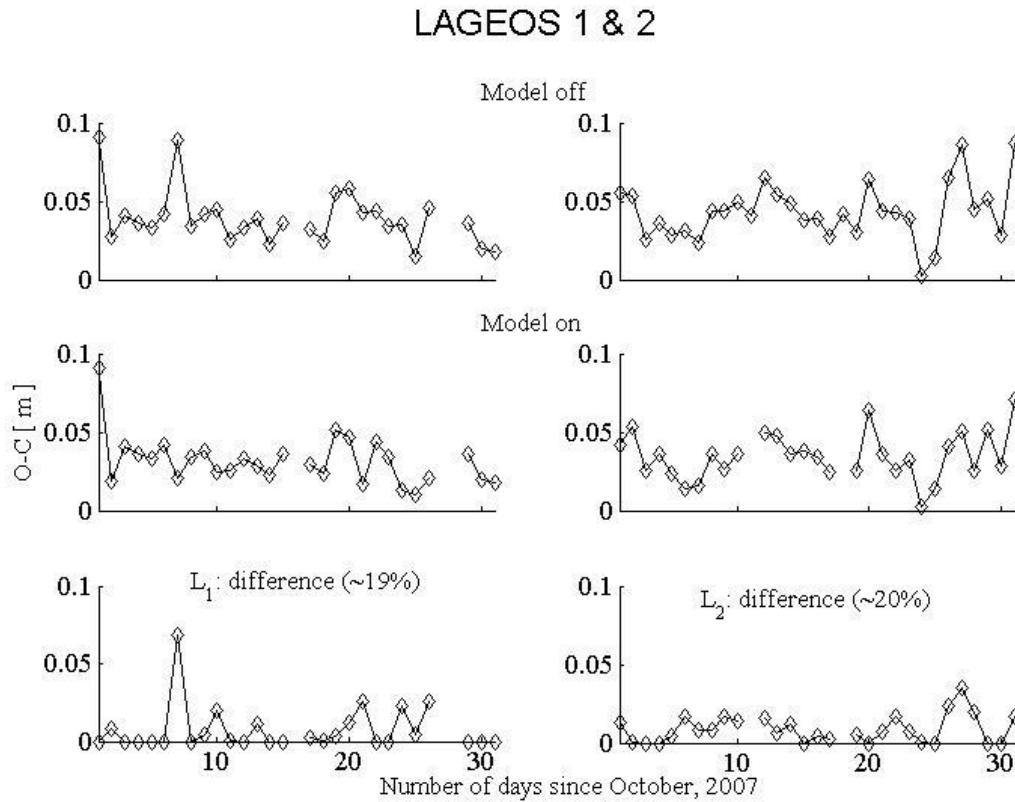


Figure 6.19. LAGEOS 1 (left column) and LAGEOS 2 (right column) observed-computed values, before (top panel), after (middle panel), percentage difference (bottom panel).

The estimated average value, minimum, maximum and standard deviation before and after incorporating the non-linear term, for O-C for LAGEOS 1 & 2 are depicted in Table 6.1.

Table 6.1. Statistical description of the observed-computed residual before and after incorporating the azimuth dependent atmospheric correction term (non-linear) in SLR processing.

Statistical parameters (O-C)	LAGEOS 1		LAGEOS 2	
	Model off	Model on	Model off	Model on
Maximum [m]	0.0908	0.0908	0.0874	0.0708
Minimum [m]	0.0145	0.0098	0.0027	0.0020
Mean [m]	0.0392	0.0317	0.0434	0.0347
Variance $\times 10^{-4}$ [m ²]	3.1121	2.4538	3.3242	2.3163

The huge improvement in O-C could be attributed to the azimuth dependent atmospheric range correction term which partly accounts for the asymmetry of the atmosphere (and the local physical conditions, such as pressure, temperature and relative humidity, along the path from the SLR station to the target satellite). Furthermore, the physical conditions (e.g., thermal radiation) of the surface in the vicinity of the SLR station will also contribute to the non-linearity and nonstationarity inherent in the SLR range. Figure 6.20 and Figure 6.21 demonstrates the azimuth dependent atmospheric range correction values based on the one-month SLR data processed by SLR analysis software developed at HartRAO.

As depicted in Figure 6.20 and Figure 6.21, there is generally strong azimuth dependence in the values. While the current one-month data might not be sufficient to demonstrate the actual quadrant dependence of the atmospheric range bias correction, the preliminary results point to specific arcs depicting non-linear relation between the angular direction and the atmospheric range correction. Furthermore, the average correction value of the present analysis is negative (see Figure 6.21), therefore suggesting that the current model used for atmospheric range correction could probably be overestimating the atmospheric range bias. This result is of extraordinary importance to the ILRS working group as well as to the research community (though long term analysis is required) with regard to the benefit of incorporating non-linear and nonstationary models in the analysis geodetic data.

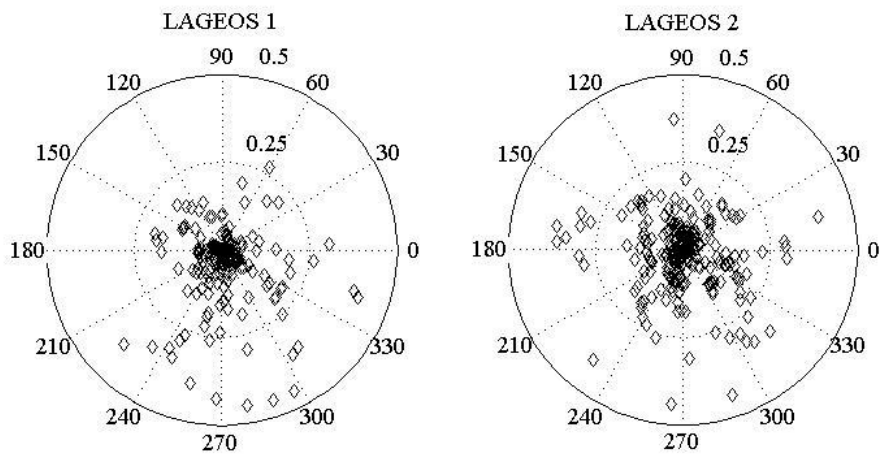


Figure 6.20. Polar description of azimuth dependent atmospheric range correction for LAGEOS 1 and 2. Only atmospheric range correction values below 0.5 (accounts for 98% of the total correction) are plotted for clarity.

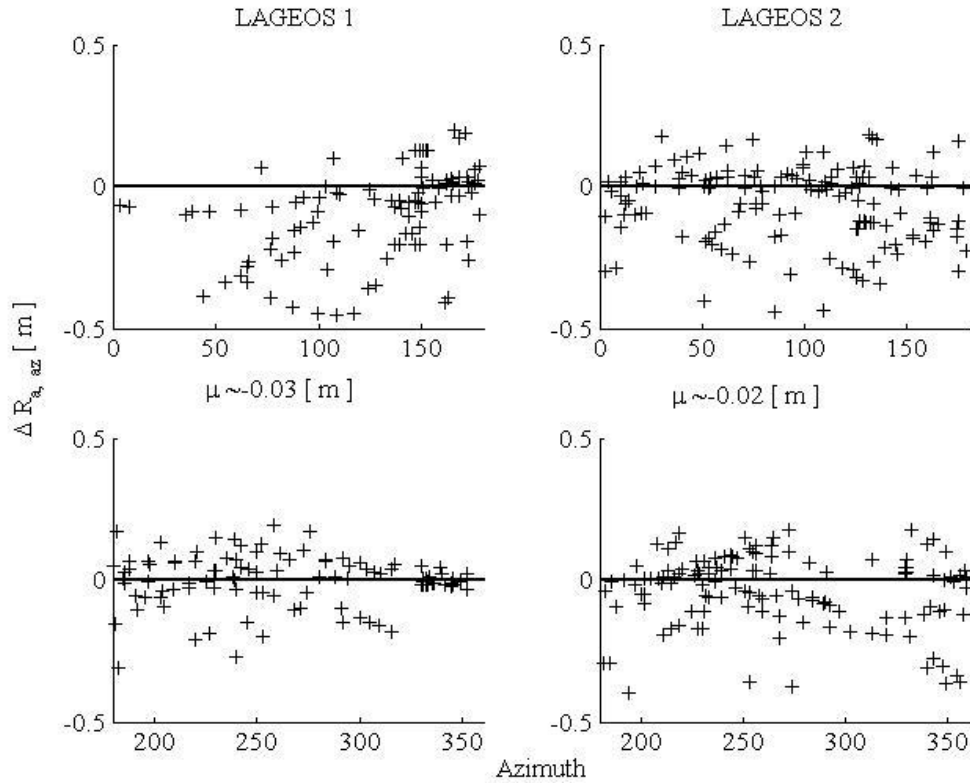


Figure 6.21. Southern (top row) and Northern (bottom row) hemisphere azimuth dependent atmosphere range correction. A negative mean value suggest that the current atmospheric range correction models generally overestimates the atmospheric range bias.

6.5. Concluding remarks

The two critical strengths for non-linear approach to the analysis of WV fluctuations are as follows:- First, they are intrinsic to the signal where in this case, linear methods have been exploited, yet certain structures in WV fluctuations have not been accounted for. Secondly, the atmospheric system is intuitively known to include non-linear components and therefore a linear description could be unsatisfactory. It is rather subjective to presuppose that the non-linear components in the atmosphere prove enough that the non-linearity is also reflected in troposphere WV fluctuations. As a result and without any prejudice, the application of non-linear analysis methods of WV fluctuations reported here was first justified by the establishment of non-linearity in WV fluctuations in the first part of this chapter.

Different non-linear approaches to the analysis have been introduced and applied to the study WV fluctuations. The DFA and wavelet based analysis tools are widely used in several fields of complexity analysis in science. For the first time however, the geodetic

troposphere WV time series has been decomposed into segments and nonstationary processes investigated using statistical information. It is shown from the wavelet space analysis that the tropospheric WV has trends and unusual magnitudes indicating nonstationarity. Further, the second-order statistical properties (means, variances and correlations) show that they are time variants. This is the additional evidence that WV variability is driven by forces that are nonstationary. The PWV time series also has self-similar and long-range dependence properties which are dependent on the WT 'detail'.

While wavelet based approach is a good tool for detection, identification and measurement of features such as scaling in the data, it is a poor method for analysing the time-energy-frequency distributions. The extracted statistical properties are vital for establishing the presence and nature of non-linear and nonstationary properties in the data. In order to accommodate the non-linear and nonstationary structures in WV fluctuations, an alternative strategy: the EMD (EEMD) is used to adaptively decompose the WV fluctuations into different scales based on the local temporal characteristic of the data. The use of EEMD enables comparison of WV and the mean troposphere temperature, thereby giving a powerful method to extract their features that could be used to describe their dependence. Such assertion has meteorological and geodetic applications.

In order to assess the contribution of incorporating non-linear/nonstationary aspects in geodetic analysis, a non-linear term which accounts for the azimuth dependent atmospheric range bias was incorporated onto the SLR analysis software developed at HartRAO. Results show that by incorporating non-linearity and nonstationarity to the atmospheric range correction model, a 15 - 20% improvement in the estimated O-C residuals derived from the analysis of one-month SLR data was achieved for the orbits of LAGEOS 1 and 2.

7. Concluding remarks

Now a whole is that which has a beginning, middle, and end.
- Aristotle, c330 BC.

Data analysis is an important tie in the scientific research cycle of observation, analysis, interpretation and theorising. In particular, time series analysis: this often entails modelling and theoretical studies, and are often required in order to understand fluctuations of tropospheric parameters such as tropospheric delay due to WV and delay gradients and WV. These parameters are used in meteorology and climate studies as well as in space geodetic applications. The research work reported in this thesis is aimed at contributing to both these fields. We have used both parametric and non-parametric tools and studied particular process properties as inferred from the variability of tropospheric parameters. This is the first attempt to systematically apply model-based and non-linear analyses strategies to investigate the dynamic structure embedded tropospheric parameters.

To summarise, the current research reports that the variability of WV and tropospheric delays due to WV over southern Africa a) exhibits multiscale properties b) are driven by non-linear and non-stationary processes, and c) over a long period of time, the fluctuations exhibit complex scaling properties, which suggest that the fluctuations have temporal memory. As a result, tropospheric geodetic parameters do not satisfy the stationary conditions. Furthermore, incorporating non-linearity and nonlinearity to the atmospheric range bias correction in SLR analysis improves the O-C residuals by more than 15%. To conclude, at various points in this thesis, we have assessed and characterised the:

a) *Stochastic behaviour of tropospheric WV or tropospheric delay due to WV*

In the course of the thesis, the previous literature on geodetic modelling of tropospheric parameters was examined. Time series analysis of tropospheric parameters by use of the automatic model-based approach was assessed in detail. The Box-Jenkins approach of automatic model identification and selection of the ARMA model, which models the dependence structure embedded in WV time series, was proposed, illustrated and analysed. It was found that if a parameter series is transformed to stationarity, then the underlying model structure could be represented by the ARMA model with model degree and order determined via the maximum likelihood criteria.

b) *Multiscale variability of WV in the low and mid-tropical Africa*

Empirical studies and simulations of WV variability over the last decade presume that the inherent fluctuations are stationary and Gaussian. The multiscale structure of WV in the low- and mid-tropical Africa region was investigated, based on *in situ* radiosonde observations of the SHADOZ station network comprising of Ascension (Ascension Island), Irene (South Africa), Reunion (Reunion) and Nairobi (Kenya) and the numerical model simulations for the period 1998 to 2006. The purpose of analysing WV fluctuations in tropical Africa was to obtain an in-depth understanding of the spatial-temporal WV fluctuations as well as to study the mechanisms driving WV variability and its link to the climatic variables. The climatic variables influenced by WV are essential for accurate geodetic tropospheric modelling. The results from the analysis show that WV exhibits high frequency fluctuations in the wavelet space. Furthermore, the embedded pattern of temporal WV fluctuations over the SHADOZ network has a dominating monthly signature. This dominant variance appears to be associated with locally-driven WV variations such as the local weather systems. The power law scaling of WV wavelet energy is a critical finding in this research. In the study, the approximate log-log linear relationship at smaller temporal scales, which breaks down at synoptic scales, suggests that the energy-times spectra of WV on different temporal scales are correlated. Furthermore, based on PCA, three dominant modes emerge. These modes explain ~ 98% of the total spatial variance of the normalised energy in WV fluctuations.

c) *Self-similar behaviour in tropospheric WV*

Studying the dynamic structure in WV or tropospheric delay caused by WV based on the wavelet approach is sufficient with regard to detection, identification and measurement of such as second order statistical parameters (which are the mean and variance) and scaling in the data. In the thesis, self-similar behaviour is assessed by use of DFA in the time-energy-frequency distributions. The extracted statistical properties are vital for establishing the presence and nature of non-linear and non-stationary properties in the data. In order to accommodate the non-linear and non-stationary structures in WV fluctuations, an EEMD is used to adaptively decompose the WV fluctuations into different scales, based on the local temporal characteristic of the data. The use of EEMD enables comparison of WV and the

mean troposphere temperature, thereby giving a powerful method to extract their features that could be used to describe their dependence.

d) Detection, characterization and incorporation of non-linearity and nonstationarity for atmospheric range bias correction in SLR analysis

The atmosphere-Earth and Ocean is an intrinsically non-linear and nonstationary physical system that is the subject of space geodetic research. This non-linearity/nonstationarity is manifested in many series of geodetic variables. The benefit of introducing non-linearity and nonstationarity in atmospheric correction, for example, to the SLR range has been assessed. In particular, a non-linear function is introduced to model the azimuth dependent atmospheric range correction. Based on the present analysis of one-month of SLR data, the azimuth dependent atmospheric range correction results suggest that introducing a second-order non-linear function could improve the O-C residuals by over 15% and the computed azimuth atmospheric range correction is generally negative suggesting that the current atmospheric range correction models could be overestimating the atmosphere range bias.

The studies in this thesis raised some outstanding questions and leads to many possible future extensions. These questions emerge from the ideas and concepts proposed in this work and therefore initiate new fields of research. An interesting perspective in this regard is the refinement of tropospheric modelling strategies so as to include the non-stationary behaviour of tropospheric WV or tropospheric delay due to WV. Geodetic analysis strategies often model tropospheric delays and delay gradients based on the concept of stationarity. However, and as can be inferred from the present work, tropospheric parameters are non-linear and non-stationary. Therefore an adjustment of tropospheric modelling strategies for geodetic applications is suggested.

The analyses of self-similar behaviour in tropospheric parameters by use of a scaling parameter have important climatic applications. In the current study, we have investigated and found that tropospheric parameters have memory. This memory has spatial dependence and therefore a global climatology of scaling parameters derived from various meteorological parameters could be an important product to climate change studies. An important research topic could therefore be the development of methodology to generate scaling parameters from various non-parametric approaches for the purpose of characterising the spatial self-similar patterns at global scales.